Bulletin of the Seismological Society of America, Vol. 81 5, pp. 1945–1957, October 1991

DIRECTIONAL SITE RESONANCES OBSERVED FROM AFTERSHOCKS OF THE 18 OCTOBER 1989 LOMA PRIETA EARTHQUAKE

BY ORNELLA BONAMASSA AND JOHN E. VIDALE

ABSTRACT

Two weeks after the 18 October 1989 Loma Prieta, California, earthquake, 18 three-component digital seismometers were deployed in the epicentral area to form three six-station subarrays. The subarray configuration allowed us to investigate the presence of direction- and frequency-dependent site resonances. We measured the shear-wave polarization from the recordings of 10 aftershocks from the Loma Prieta earthquake.

Our observations show that the site response has a strong azimuthal dependence and that both the shear-wave polarization and the spectral amplitude of the ground motions are affected by site characteristics. In the frequency range from 1 to 18 Hz, the majority of stations examined showed preferred azimuths of ground motion for the scattered waves that did not depend either on the earthquake location or on the polarization of the shear waves expected from the known focal mechanism. The measurements were made from 5-sec windows that included direct and scattered shear waves, which contain the largest amplitude motions in the near-source region and are therefore of most interest to earthquake engineers. However, in the 0- to 2-Hz frequency range, the first pulse of shear waves shows a polarization that is well predicted by the mechanism and location of the earthquake.

The rapid spatial variation of the preferred directions and their corresponding frequencies indicate that geologic structures within a distance of the order of 50 m probably control these site effects. We suggest that the site amplified the motion of scattered waves in one preferred direction, altering the resulting polarization and modulating the spectral amplitude.

INTRODUCTION

The analysis of strong ground motions recorded at various surficial sites (Seed *et al.*, 1976; Campbell, 1981; Joyner and Boore, 1981; Rogers *et al.*, 1984; Kagami *et al.*, 1986) and in boreholes (Haukkson *et al.*, 1987; Malin *et al.*, 1988) shows that near-receiver geology is an important factor in determining the strength of shaking from an earthquake. Spectral analysis of time histories recorded at the same site for Italian earthquakes has shown amplification (or deamplification) in specific frequency bands that is independent of earthquake location and that is not reproduced at neighboring sites (Rovelli *et al.*, 1988). On the basis of observations such as these, the sum of the complex phenomena that take place near the receiver has been termed the *site effect.* Although both source and site effects strongly influence observed spectral amplitudes, it is still possible to distinguish between the two effects (e.g., Andrews, 1984; Castro *et al.*, 1990; Mueller and Bonamassa, manuscript in preparation).

In many cases, flat-layered receiver structure has been useful in explaining observed site amplification (e.g., Seed *et al.*, 1972; Joyner *et al.*, 1976). The amplification of 2-sec energy by lakebed deposits in Mexico City during the 1985 Michoacán earthquake is a dramatic example of the influence of thin low-velocity layers near the Earth's surface (Campillo *et al.*, 1989). Patterns of amplification and duration of shaking on the surface that require lateral variations in geologic structure (Vidale and Helmberger, 1988), and strong-motion effects of some simple large-scale structures (Vidale *et al.*, 1985; Bard and Gariel, 1986; Kawase and Aki, 1989) have been investigated; however, the importance of near-receiver structures more complicated than horizontal layers has not been previously documented for high-frequency seismic energy.

The aim of our study is to investigate the presence of direction- and frequency-dependent station resonances. Previous work on the 1987 Whittier Narrows, California, earthquake sequence suggests that the *strength* of the shaking at a site partly depends on the focal mechanism (Vidale, 1989), but this study indicates that in many cases the *direction of polarization* of the motion depends on the site geology. We show that in the frequency range from 1 to 20 Hz, some sites have preferred directions of ground motion polarization that do not depend either on the earthquake location or on the polarization of the shear waves expected from the focal mechanism. The most likely explanation for these azimuthal patterns is that particle motion in one direction is amplified compared to the motion in the orthogonal direction. The observations that these amplifications can change on a scale of 25 m and that the preferred directions of motion remain relatively constant through the *S*-wave arrival and coda suggest that these structures are very near the receivers, probably within distances of the order of 50 m. It is of great interest to earthquake engineers whether particular sites are likely to be strongly shaken in particular directions in a given frequency range. Our observations are not explicable by the conventional azimuthally symmetric models of site response.

Data Analysis

The analysis performed in this article is based on data collected with the instruments provided by the IRIS-PASSCAL Loma Prieta Aftershock Project. During the first 2 weeks after the 18 October 1989 Loma Prieta earthquake, 21 stations, each consisting of one Reftek 16-bit digitizer and two L-22 three-component geophones (resonance frequency is 2 Hz), operated in the epicentral region. For the following 3 weeks, nine of these instruments were reconfigured to form three six-station, three-component subarrays (for a total of 18 recording sites) to allow a detailed study of ground motions (see Fig. 1). The geometry of the subarrays was designed to be favorable for the analysis of the spatial and frequency coherence of the shaking. Figure 2 shows the location of the sensors at the ZAYA array whose records we examined in detail in this article.

Ten aftershocks characterized by varying locations and differing focal mechanisms (see Table 1) were selected for analysis. All events have an excellent signal-to-noise ratio and clear initial *P*-wave onsets and were recorded by all six stations installed at the ZAYA array.

This study is focused on the ZAYA site, but a preliminary analysis of data from the two other array sites shows similar levels of site effects at the PREZ array and less severe site effects at the WVRD array. A typical suite of the north–south component seismograms for all six elements of the ZAYA array is shown in Figure 3. It is remarkable that even the instruments spaced only 25 m apart record noticeably different signals.

Our analysis of site effect is based on both the polarization and spectral amplification of shear waves at the stations of the ZAYA array. On each seismogram, a cosine-tapered 5-sec window is applied in order to analyze both

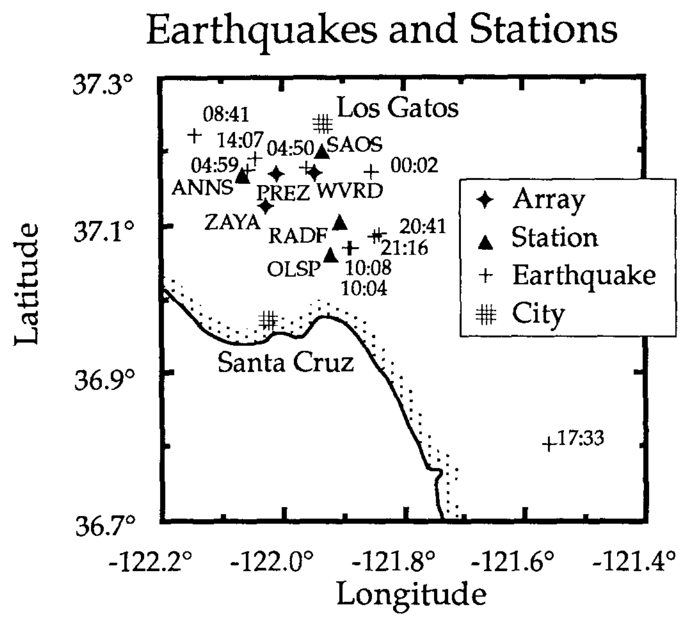

FIG. 1. Map view of the IRIS-PASSCAL stations and earthquake locations used in the analysis. Earthquake locations were obtained from David Oppenheimer (personal comm.).

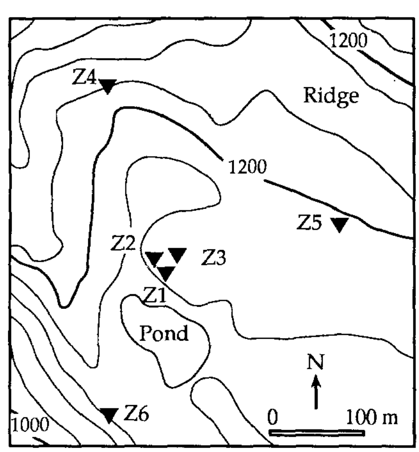

FIG. 2. Location of the six three-component stations comprising the ZAYA array. The array has the geometry of an inner and an outer triangle whose sides are approximately 25 and 300 m, respectively.

direct and scattered shear waves. The use of the 5-sec window for earthquakes having source duration less than 1 sec is justified by the need to study the part of the seismogram that shows the strongest shaking. If strong shaking lasts less than 5 sec, the polarization analysis is weighted by the square of the amplitude of shaking and therefore is dominated by the time intervals that have strong shaking. The spectra used below are an rms of the amplitude spectra of the two horizontal components. For each event, an average spectrum is computed by a logarithmic average of the spectra at all triggered stations, excluding the

TABLE 1
EARTHQUAKE PARAMETERS

Day	Time	Latitude	Longitude	Depth (km)	Δ (km)	Magnitude	Dip Direction*	Dip	Rake
11-14-89	00:02	37°10′	−121°51′	3.7	17	1.9	145°	80°	50°
11-14-89	04:50	37°11′	−121°58′	6.0	7	2.3	215°	40°	130°
11-14-89	08:41	37°13′	−122°09′	8.4	16	2.0	230°	30°	120°
11-14-89	17:33	37°48′	−121°34′	7.1	58	3.1	90°	15°	−130°
11-14-89	20:41	37°05′	−121°50′	5.7	19	2.8	220°	358°	100°
11-14-89	21:16	37°05′	−121°51′	5.6	20	3.4	165°	50°	10°
11-15-89	10:04	37°04′	−121°53′	15.0	15	2.5	275°	40°	−50°
11-15-89	10:08	37°04′	−121°53′	14.8	16	2.3	260°	35°	−50°
11-16-89	04:59	37°11′	−122°03′	10.8	5	2.9	240°	45°	160°
11-16-89	14:07	37°12′	−122°03′	10.5	5	2.4	200°	65°	100°

*The dip direction is the strike direction increased by 90°.
Mechanisms were provided by D. Oppenheimer (personal comm.).

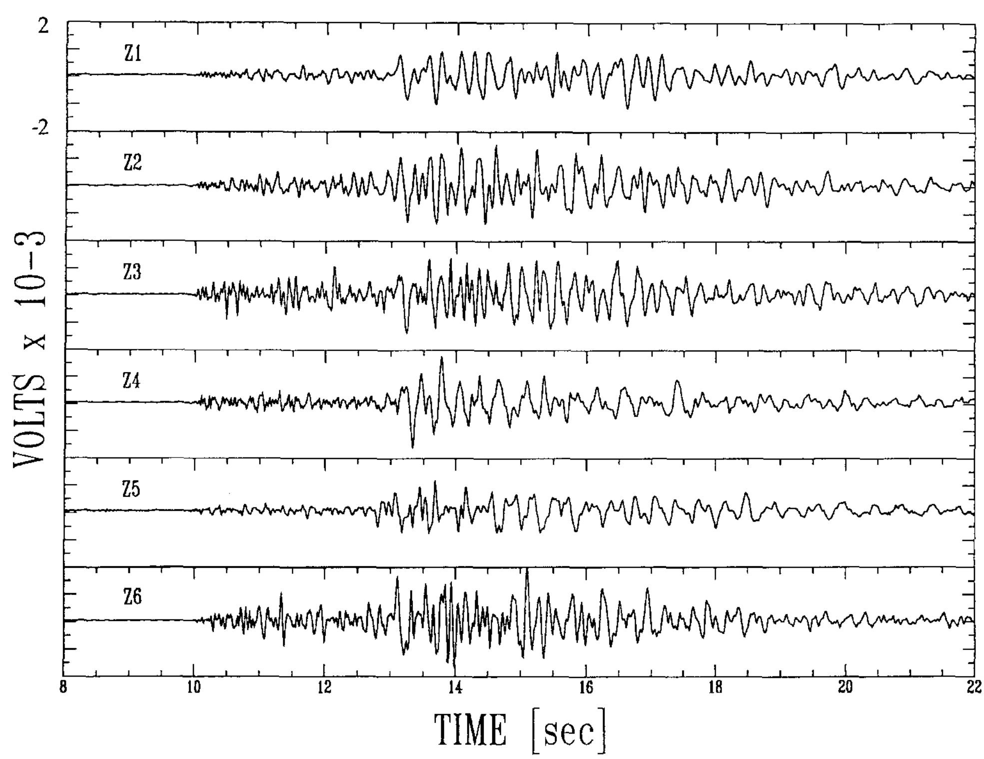

FIG. 3. North-south component seismograms for all six elements of the ZAYA array. The top three seismograms were recorded at the inner sites spaced 25 m apart; however signals are noticeably different.

stations of the ZAYA array. In this way, azimuthal amplitude variations and site effects have been averaged, providing a spectrum characteristic of the event. We did not correct for instrumental response, geometrical spreading, focal mechanism, or attenuation along the path. With logarithmic averaging, geometric spreading corrections would only shift the baseline of the spectra, not change the patterns shown. Attenuation appears to depend on the path in unpredictable ways; this may be the subject of future studies. We note, however, that some studies have inverted for attenuation (e.g., Castro *et al.*, 1990).

Spectral amplitude ratios are computed between each of ZAYA's six stations and the average event spectrum at frequencies of 1 to 20 Hz. Ratios estimated for each event are averaged for the 10 events considered and are shown in Figure 4. This figure compares the average spectral amplitude of ZAYA's stations to the rest of the network. A value of the ratio equal to one would represent spectral behavior similar to the rest of the stations; in general, some amplification is seen. An increase in the ratio in two distinct frequency ranges is evident: at low frequency between 2 and 7 Hz for all stations, and at high frequency between 13 and 18 Hz for some stations. The amplitude ratios for the inner three elements are similar at 6 Hz and lower frequencies; the outer elements are similar only below 3 Hz.

The primary goal of this analysis is to investigate directional site effects and to determine their consistency and strength. A site effect that introduces a consistent amplification of one component of the motion will be most easily recognizable in a polarization study. Therefore, we have performed a systematic estimate of shear-wave polarization direction at different frequencies for many earthquakes with various locations and mechanisms recorded at the stations of the ZAYA array. Cosine-bell-shaped 2-Hz-wide windows centered from 1 to 20 Hz have been applied in the frequency domain as bandpass filters in overlapping frequency bands. Polarization directions have been estimated from the covariance matrix of the real signal. The eigenvector associated with the largest eigenvalue points in the direction of the largest amount of ground motion: this direction is indicated in this article as the polarization direction (Montalbetti and Kanasewich, 1970; Vidale, 1986). In order to eliminate scattered compressional waves from the analysis of shear-wave polarization, we have estimated

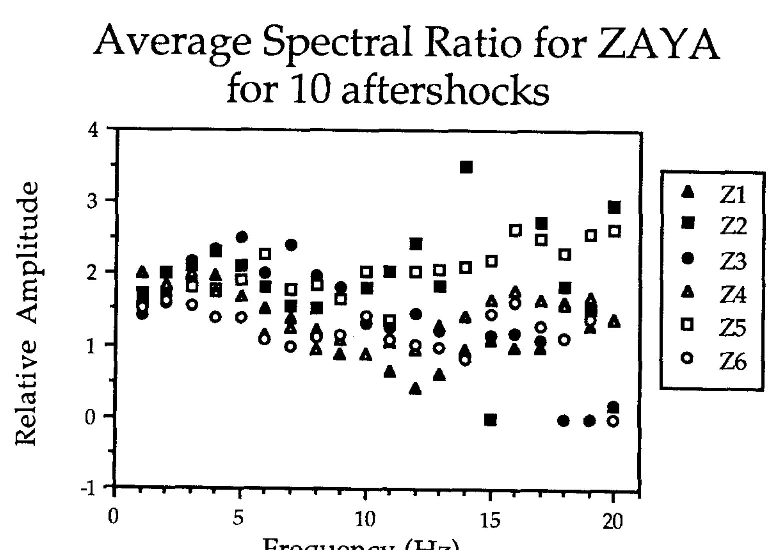

FIG. 4. Average spectral ratios for the six elements of the ZAYA array. Solid symbols are from the inner elements, open symbols from the outer elements.

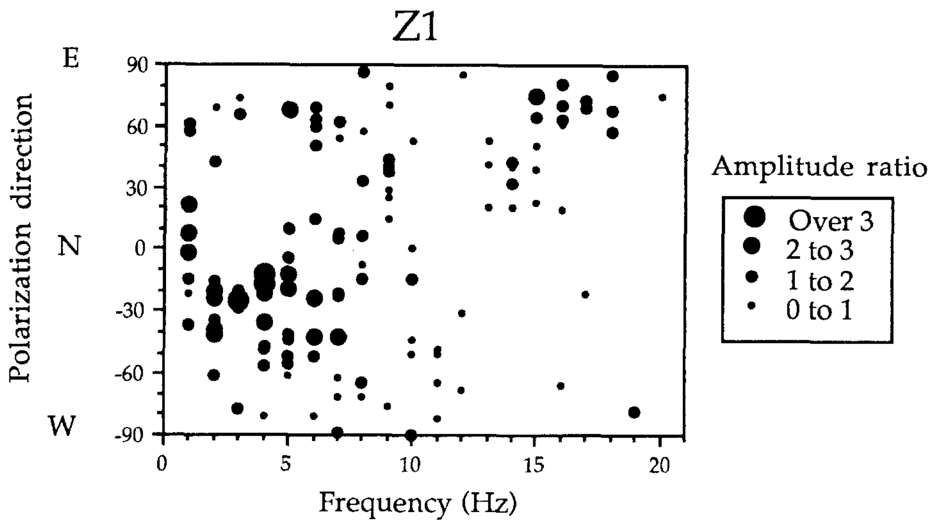

FIG. 5. Direction of strongest polarization plotted against frequency for the station Z1. Data from 10 events are shown. The symbol size is proportional to the amplification relative to the average spectra computed from stations outside the ZAYA array. The polarization has a range of 180°; the range extends from east to west through north. Thus, the polarization direction wraps from the top of the plot to the bottom.

the dip angle of each filtered signal. Data having polarization dips larger than 25° from the horizontal are most likely due to late *P*-wave coda, which we verified by inspecting the time domain records, and have been discarded. This selection has reduced the number of polarization measurements available at frequencies higher than 10 Hz.

RESULTS

The polarization direction versus frequency at station Z1 is shown in Figure 5 for the 10 events analyzed. In the hypothesis that the polarization is controlled exclusively by the focal mechanism at all frequencies, we would expect the polarization to have a certain azimuth at 1 Hz and to maintain that azimuth for all frequency bands. Plotting together the angles estimated for 10 different events for the range of frequencies, we would expect the angle values not to change with frequency for the same site for a given event, with each event showing a different direction of shaking. Instead, we see that in the frequency range from 2 to 5 Hz, most events produce particle motion with an azimuth of about −20° (N20°W) in correspondence with the spectral amplification seen in Figure 4 for this station. The spectral amplification may also be seen in the clustering of the largest symbols near −20° at 22 to 4 Hz. Perhaps some alignment at the azimuth 70° is seen for frequencies from 15 to 18 Hz. The similarity of particle motion directions for the 10 events, despite differences in focal mechanisms, suggests that the geologic structure that is amplifying motion at 2 to 5 Hz is more complicated than a simple stack of flat layers. Our interpretation of Figure 5 is that ground motion at site Z1 in the 2- to 5-Hz range is most prone to strong shaking with an azimuth of −20°, and the particle motion carries little information about the focal mechanism, with the exception of the first 0.5 sec, as noted below.

That this directionality is significant may be seen in Figure 6, which shows the horizontal particle motion of the ground in the passband from 3 to 5 Hz. The ratio of amplitude in the direction of strongest shaking (generally N20°W) to the amplitude in the orthogonal direction ranges from 1.4 to 2.5 and averages 1.8. The ratio of 1.8 in amplitude means a ratio of 3.2 in the energy of shaking, which may be significant to engineers.

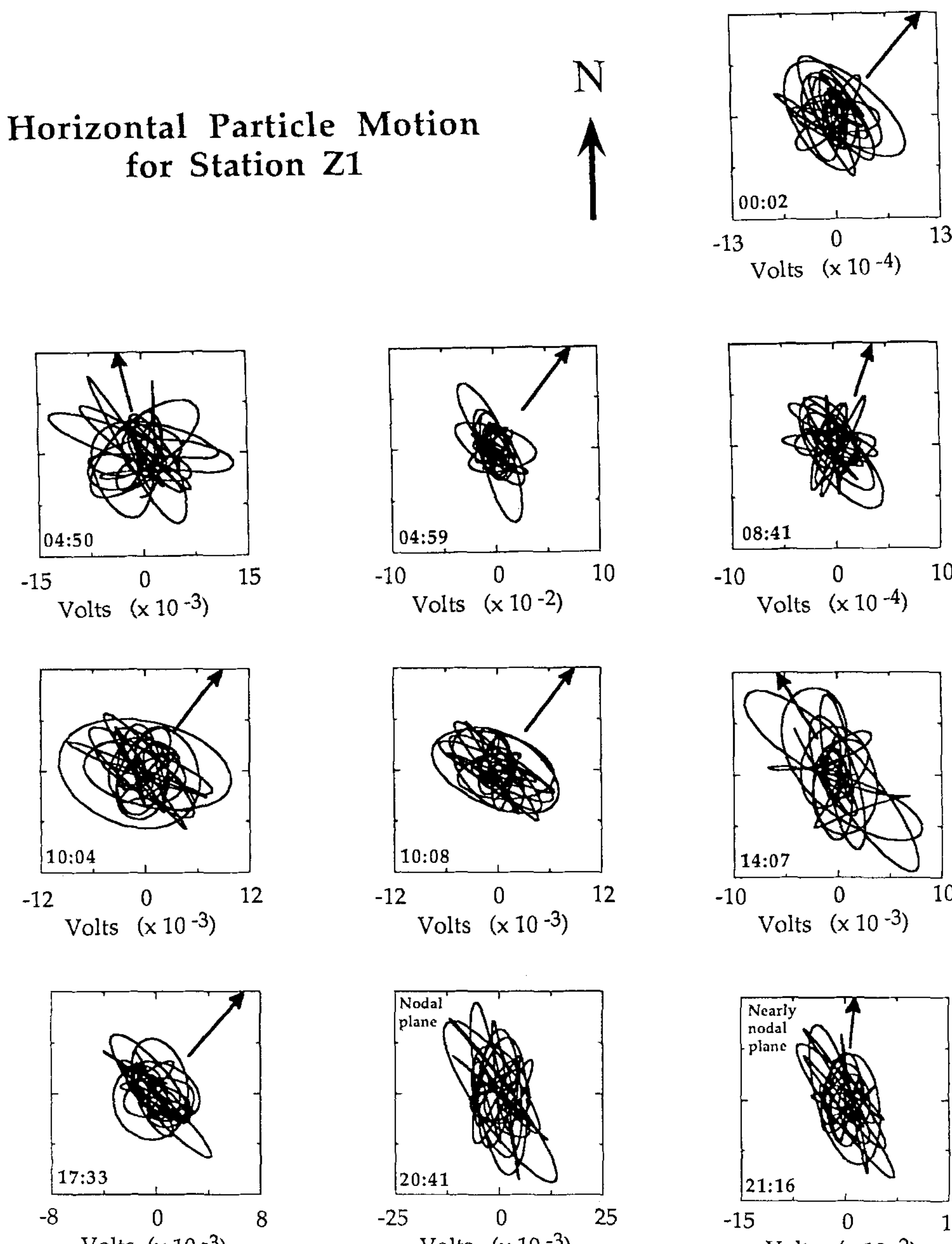

FIG. 6. Horizontal particle motion in a 5-sec window that starts with the shear-wave arrival for station Z1. Data are filtered in the passband from 3 to 5 Hz. The arrows point in the polarization direction predicted by the focal mechanism. The events are specified by hour and minute in the *lower left* corner of each frame.

Four of the six elements in the ZAYA array show strongly preferred S-wave particle motion directions in some frequency bands. Plots for station Z2 to Z6 are shown in Figure 7. Station Z2 shows a preferred direction of motion that shifts continuously clockwise from about 0° toward 90° with increasing fre-

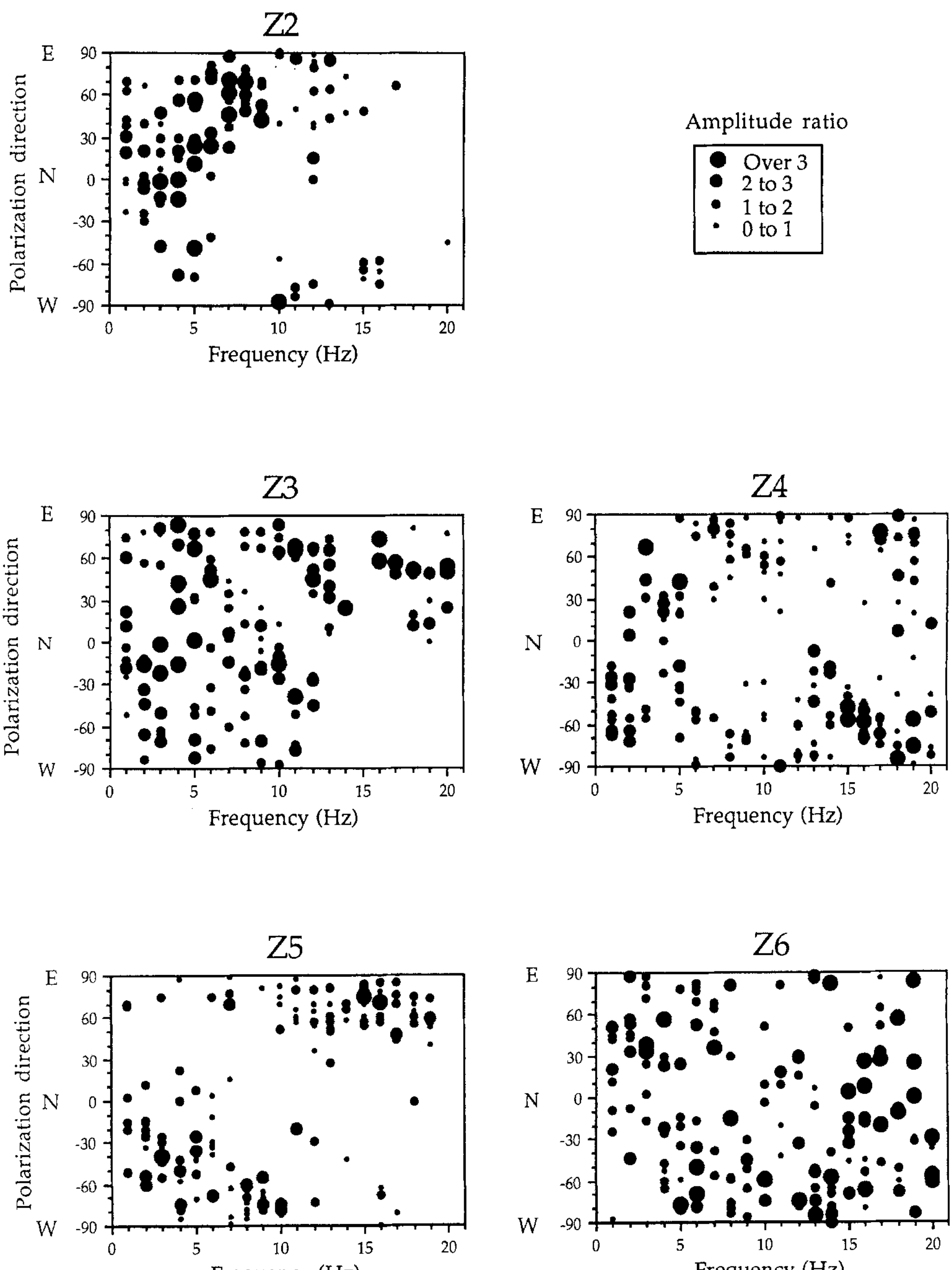

FIG. 7. Direction of strongest polarization plotted against frequency for the stations Z2 to Z6. Data from 10 events are plotted. The symbol size is proportional to the amplification relative to the average spectra computed from stations outside the ZAYA array.

quency. Stations Z3 and Z6 show no strong direction-dependent patterns, however neither do they show agreement with the direction expected from the locations and focal mechanisms. Station Z3 may show the more traditional direction-independent amplification at 3 to 5 Hz, consistent with the expected results from a flat-layered structure. Station Z4 shows motions centered around $-45°$ at 1 Hz and a strong $-60°$ clustering and amplification at 15 Hz. This behavior differs strongly from 1-Hz observations at the inner stations that show a preferred direction for the polarization in the positive range. Thus, the amplitude at 1 Hz is similar across the array, as seen in Figure 4, but the polarization directions at 1 Hz vary, as seen in Figures 5 and 7. Station Z5 shows particle motion orientation that rotates counterclockwise from 0° to $-90°$ in the frequency range from 1 to 10 Hz.

The estimated polarization directions are due to the strongest shaking in the 5-sec windows and apparently carry little information about the source. A closer examination of the seismograms allows us to formulate an interpretation of the observed phenomenon.

Figure 8a shows the seismograms of the event of 14 November 1989 at 00:02 GMT (same event shown in Fig. 3, details are given in Table 1) recorded by the six sensors of the ZAYA array. The top traces are the stack of the recordings shown below. For each sensor, two horizontal components are plotted: the upper trace is in direction of the polarization consistent with the focal mechanism; the lower is in the orthogonal direction. Data have been filtered with a passband of 0 to 2 Hz. The component in the direction of the expected polarization starts with a 0.5-sec pulse, followed by a scattered coda characterized by a lower amplitude. The orthogonal component is quiet at the time of the pulse, but it shows a series of scattered waves in the coda whose amplitude is comparable with the coda on the other component. This phenomenon is evident for all the six sensors, confirming that the polarization direction of the first 0.5-sec pulse is consistent with the polarization direction predicted by the focal mechanism. This initial coherence is expected (see Bernard and Zollo, 1989, for a review; Menke *et al.*, 1990). Figure 8b shows the same data, but bandpass filtered between 3 and 5 Hz, where the directional resonance is observed for station Z1. Various stacking strategies were tried, but the 3- to 5-Hz energy simply does not stack well. As in the previous figure, the first pulse is present in the top seismogram recorded at Z1 and is almost absent in the orthogonal component. The coda, however, shows peak amplitudes larger than in the first 0.5-sec of the signal. This coda can be interpreted as a resonance effect that generates the strongest shaking of the signal and whose directional dependence is evident in the analysis of the polarization.

The focal mechanism can also be observed in the average polarization of the array in the low-frequency passband (0 to 2 Hz). Figure 9 shows the comparison between the polarization direction predicted by the focal mechanism and the polarization direction obtained by averaging the 0- to 2-Hz covariance matrix of the six sites at ZAYA array (Jurkevics, 1988). Aside from the case of observations predicted to be nodal, the agreement between focal mechanism and average array polarization is quite good.

The physical cause of this resonance effect may be topography and surface geology, given the lack of information available about the detailed structure beneath the sensors. The six sensors lie at the two sides of the San Lorenzo syncline in a geologically homogeneous area of Tertiary age. The surface

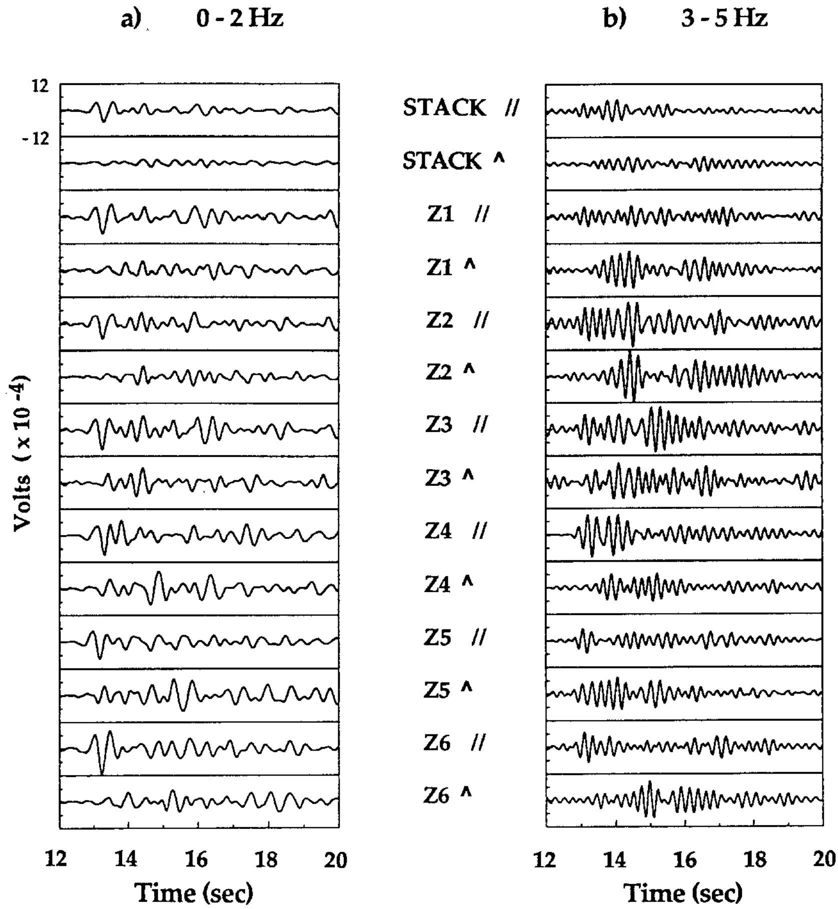

FIG. 8. Data from the 14 November 1989 (00:02 GMT) aftershock. The horizontal component seismograms recorded at the six sites of the ZAYA array have been rotated in the direction of polarization expected from the focal mechanism and in the orthogonal direction. (a) The data have been filtered in the 0- to 2-Hz passband. The *top* two seismograms are the stack of the six two-component data shown below. (b) Same as (a), except that the seismograms have been filtered in the 3- to 5-Hz passband.

geology indicates that the sensors Z1, Z2, Z3, Z4, and Z5 have been buried in Lambert Shale (Marine semi-siliceous shale and siltstone; Saucesian stage, late Miocene), while sensor Z6 is in the slightly older Vaqueros Sandstone (Marine arkosic sandstone; minor siltstone; Saucesian and Zemorrian stages, Brabb and Dibblee, 1979). Surface geology and topography are similar for the three inner sensors, leaving the observed differences unexplained. The sensor Z4, located on a steep slope near a ridge, resonates with directions that are not easily related to topography, while sensor Z6 lies on a steepest ridge and does not show a well-defined site effect. In sum, observations are not easily related to topography, while geology probably plays a significant role.

Figure 10 summarizes our results. For each station, the arrows indicate the direction of polarization and its frequency band. In general, sites that exhibit some directional effect show resonance at low frequency (1 to 3 Hz) in the northwest–southeast direction and at higher frequency in the east-west direc-

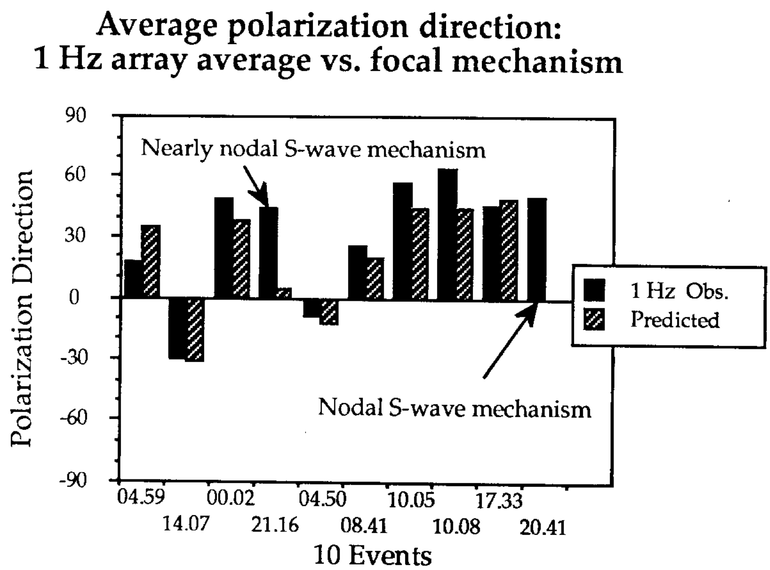

FIG. 9. Comparison between polarization direction predicted by the focal mechanism and the polarization direction obtained by averaging the covariance matrix of the six sites at the ZAYA array in the 0- to 2-Hz band.

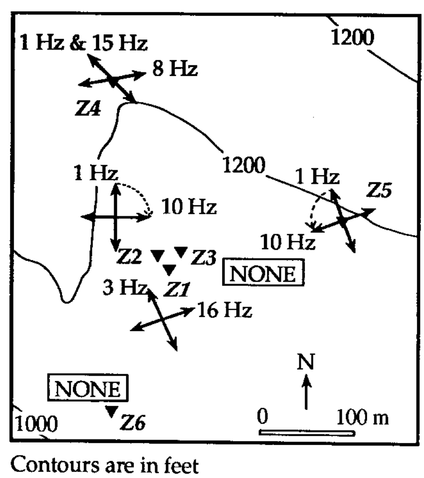

FIG. 10. Map of the ZAYA array displaying a summary of the observed directional resonances. At each site, the arrows indicate direction of the resonance and its frequency band.

tion. We will not attempt to interpret this probably coincidental correlation here.

The most likely explanation for the observed resonance patterns is that particle motion in selected frequency bands is amplified in particular directions compared to motions in other directions. The specific geological structures that cause this amplification are not yet known. The direction of amplified particle motion changes across the inner 25-m triangle of stations, and the preferred directions of motion at each station remain relatively constant through the S-wave arrival and coda.

Conclusions

The analysis of 10 events recorded at a small-aperture array of six digital stations has shown that polarization, as well as spectral amplitude of the ground motion, can be affected by site characteristics. Similar directional site resonances have also been noticed by the authors for the 1 October 1987 Whittier Narrows earthquake (Vidale *et al.*, 1991). We suggest that the site may amplify the motion in one preferred direction, leaving the motion in the orthogonal direction unaffected or diminished. This direction-dependent amplification alters the particle motion. However, the first 0.5-sec pulse of the recorded signals often shows a polarization direction consistent with the polarization direction predicted by the focal mechanism. The observation of a directional resonance is new, while site-specific spectral amplifications have previously been widely observed.

The specific geological structures that cause this amplification are not yet known. Lateral gradients in near-surface shear-wave velocity are the most likely cause of these lateral resonances. The observations that these amplifications can change on a scale of 25 m and that the preferred directions of motion remain relatively constant through the *S*-wave arrival and coda suggest that these structures are very near the receivers, probably within a few tens of meters. The predictability of the preferred direction of strong shaking should prove useful to earthquake engineers.

Acknowledgments

We wish to thank all who helped with field operations, especially Susan Schwartz, Aaron A. Velasco, Marino Protti-Quesada (UCSC), Grant Lindley and Keith Dinger (UCSB). We also thank David Oppenheimer (USGS) for providing locations and focal mechanism solutions and IRIS for supplying instrumentation for the field deployment. This material is based upon work supported by the Incorporated Research Institutions for Seismology under their Cooperative Agreement No. EAR 84-19149 with the National Science Foundation.

Support for this work has been provided in part by a grant from the W. M. Keck Foundation, and the Institute of Tectonics, University of California, Santa Cruz. Support has also been provided by the USGS grant number 14-08-0001-G1837. Contribution Number 84 from the Charles F. Richter Seismological Laboratory at the University of California, Santa Cruz.

References

Andrews, J. (1984). Objective determination of source parameters and similarity of earthquakes of different size, in *Earthquake Source Mechanics*, S. Das, J. Boatwright, and C. H. Scholz (Editors) American Geophysical Monograph 37, 259–267.

Bard, P.-Y. and J. C. Gariel (1986). The seismic response of two-dimensional sedimentary deposits with large vertical velocity gradients, *Bull. Seism. Soc. Am.* **76**, 343–60.

Bernard P. and A. Zollo (1989). Inversion of near-source *S* polarization for parameters of double-couple point sources, *Bull. Seism. Soc. Am.* **79**, 1779–1809.

Brabb, E. E. and T. W. Dibblee (1979). Preliminary geologic map of the Castle Rock Ridge quadrangle. Santa Cruz and Santa Clara counties, California, *U. S. Geol. Surv. Open-File Rep.* **79-659**.

Campbell, K. W. (1981). Near-source attenuation of peak horizontal acceleration, *Bull. Seism. Soc. Am.* **71**, 2039–2070.

Campillo, M., J. C. Gariel, K. Aki, and F. J. Sánchez-Sesma (1989). Destructive strong ground motion in Mexico City: source, path and site effects during the great 1985 Michoacán earthquake, *Bull. Seism. Soc. Am.* **79**, 1718–1734.

Castro, R. R., J. G. Anderson, and S. K. Singh (1990). Site response, attenuation and source spectra of *S*-waves along the Guerrero, Mexico subduction zone, *Bull. Seism. Soc. Am.* **80**, 1481–1503.

Haukkson, E., T.-L. Teng, and T. L. Henyey (1987). Results from a 1500 m deep, three-level downhole seismometer array, *Bull. Seism. Soc. Am.*, **77**, 1883–1904.

Joyner, W. B. and D. M. Boore (1981). Peak horizontal acceleration and velocity from strong-motion records from the 1979 Imperial Valley, California earthquake, *Bull. Seism. Soc. Am.*, **47**, 2011-2038.

Joyner, W. B., R. E. Warrick, and A. A. Oliver, III (1976). Analysis of seismograms from a downhole array in sediments near San Francisco Bay, *Bull. Seism. Soc. Am.* **66**, 937-958.

Jurkevics, A. (1988). Polarization analysis of three component array data, *Bull. Seism. Soc. Am.* **78**, 1725-1743.

Kagami, H., S. Okada, K. Shiono, M. Oner, M. Dravinski, and A. K. Mal (1986). Observation of 1-5 second microtremors and their application to earthquake engineering. Part III. A two-dimensional study of site effects in the San Fernando Valley, *Bull. Seism. Soc. Am.* **76**, 1801-1812.

Kawase, H. and K. Aki (1989). A study on the response of a soft basin for incident *S*, *P*, and Rayleigh waves with special reference to the long duration observed in Mexico City, *Bull. Seism. Soc. Am.* **79**, 1361-1382.

Malin, P. E., J. A. Waller, R. D. Borcherdt, E. Cranswick, E. G. Jensen, and N. Van Schaak (1988). Vertical seismic profiling of Oroville microearthquakes: velocity spectra and particle motion as a function of depth, *Bull. Seism. Soc. Am.* **78**, 401-420.

Menke, W., A. L. Lerner-Lam, B. Dubendorff, and J. Pacheco (1990). Polarization and coherence of 5 to 30 Hz seismic wave fields at a hard-rock site and their relevance to velocity heterogeneities in the crust, *Bull. Seism. Soc. Am.* **80**, 430-449.

Montalbetti, J. R. and E. R. Kanasewich (1970). Enhancement of teleseismic body phases with a polarization filter, *Geophys. J. R. Astr. Soc.* **21**, 119-129.

Rogers, A. M., R. D. Borcherdt, P. A. Covington, and D. M. Perkins (1984). A comparative ground response study near Los Angeles using recordings of Nevada nuclear tests and the 1971 San Fernando earthquake, *Bull. Seism. Soc. Am.* **74**, 1925-1949.

Rovelli, A., O. Bonamassa, M. Cocco, M. Di Bona, and S. Mazza (1988). Scaling laws and spectral parameters of the ground motion in active extensional areas in Italy, *Bull. Seism. Soc. Am.* **78**, 530-560.

Seed, H. B., H. Boulton, P. Schnabel, and J. Lysmer (1972). Modification of seismograph records for effects of local soil conditions, *Bull. Seism. Soc. Am.* **62**, 1649-1664.

Seed, H. B., C. Ugas, and J. Lysmer (1976). Site-dependent spectra for earthquake-resistant design, *Bull. Seism. Soc. Am.* **66**, 221-244.

Vidale, J. E. (1986). Complex polarization analysis of particle motion, *Bull. Seism. Soc. Am.* **76**, 1393-1406.

Vidale, J. E. (1989). Influence of focal mechanism on peak accelerations for the Whittier Narrows, California, earthquake and an aftershock, *J. Geophys. Res.* **94**, 9607-9615.

Vidale, J. E., O. Bonamassa, and H. Houston (1991). Directional site resonances observed from the 1 October 1987 Whittier Narrows, California, earthquake and the 4 October aftershock, *Earthquake Spectra* **7**, 107-125.

Vidale, J. E. and D. V. Helmberger (1988). Elastic finite-difference modeling of the 1971 San Fernando, California, earthquake, *Bull. Seism. Soc. Am.* **78**, 122-142.

Vidale, J. E., D. V. Helmberger, and R. W. Clayton (1985). Finite-difference seismograms for *SH* waves, *Bull. Seism. Soc. Am.* **75**, 1765-1782.

INSTITUTE OF TECTONICS
UNIVERSITY OF CALIFORNIA
SANTA CRUZ, CALIFORNIA 95064

Manuscript received 29 July 1990